Preparation of Plate-Form Manganese Oxide by Selective Lithium Extraction from Monoclinic Li_2MnO_3 under Hydrothermal Conditions

Weiping Tang*

Research Institute for Solvothermal Technology, 2217-43, Hayashi-cho, Takamatsu 761-0301, Japan

Hirofumi Kanoh, Xiaojing Yang, and Kenta Ooi

Shikoku National Industrial Research Institute, 2217-14, Hayashi-cho, Takamatsu 761-0395, Japan

Received May 3, 2000. Revised Manuscript Received July 31, 2000

Hydrothermal lithium extraction from well-crystallized Li_2MnO_3 crystals was studied by scanning electron microscopy (SEM) observation, chemical, and X-ray diffraction analyses. Monoclinic Li_2MnO_3 polyhedral crystals were prepared in an LiCl flux at 650 °C. The lithium extraction was carried out in a variety of H_2SO_4 solutions with mole ratios of H^+ in the solution to Li^+ in the solid ($[H^+]_l/[Li^+]_s$) of 0.1, 0.15, 0.25, 0.50, 0.75, and 1.0 under a hydrothermal condition at 140 °C. The lithium extraction from Li_2MnO_3 proceeds consuming equimolar H^+ in the solution by the mechanism of a Li^+/H^+ ion exchange reaction when $[H^+]_l/[Li^+]_s \leq 0.15$ and by the mechanism of a mixture of the Li^+/H^+ ion exchange reaction and lithium dissolution when $0.25 \leq [H^+]_l/[Li^+]_s \leq 0.75$. The lithium-extracted phase preserves the crystal structure of Li_2MnO_3 with a partial contraction of the lattice when $0.25 \leq [H^+]_l/[Li^+]_s \leq 0.75$. SEM observation showed that the lithium extraction brings about a cleavage of the Li_2MnO_3 particle along the (001) plane to result in a unique form in which platelike particles are stacked, preserving the polyhedral outline. High-magnification SEM observation showed that the platelike particles consist of an aggregate of subplates with nanometer thickness in parallel arrangement. Slit-shaped mesopores were formed among the subplates. γ-MnO_2 was formed as a final product when $[H^+]_l/[Li^+]_s = 1$. A structural model is proposed to explain the mechanism of lithium extraction as well as the cleavage of the particle.

Introduction

The extraction of metal ions from manganese oxides with ultramicro- or micropores proceeds topotactically without any change in crystal structure. Manganese oxides' adsorptive properties depend largely on their crystal and pore structures.[1−7] For example, the spinel-type manganese oxide with a [1 × 3] tunnel network of [MnO_6] octahedra,[1−4] the hollandite type with a [2 × 2] tunnel,[5] the birnessite type with a [2 × ∞] layer, and the todorokite type with a [3 × 3] tunnel show selective adsorption for lithium, potassium, rubidium, and cesium ions,[6,7] respectively. These properties make manganese oxides not only excellent selective adsorbents but also excellent cathode materials for advanced lithium batteries[8−10] and electrodes for selective electroinsertion of metal ions.[11,12] Recently, rock-salt-type lithium manganese oxides with a layered structure similar to $LiCoO_2$ have attracted attention because of their high capacity and stability as materials for lithium adsorption or for a lithium rechargeable battery. Layered $LiMnO_2$ prepared from fluxing α-$NaMnO_2$ with LiX (X = Cl and Br) in *n*-hexanol around 150 °C has been reported to have a high discharge capacity of 270 mA·h/g at the first discharge process.[13] The layerlike compound Li_2MnO_3 is a promising precursor.[14−20] The products obtained by

* To whom correspondence should be addressed. E-mail: tang@ktz.or.jp.

(1) Vol'Khin, V. V.; Leont'eva, G. V.; Onolin S. A. *Neorg. Mater.* **1973**, *6*, 1041.
(2) Shen, X. M.; Clearfield, A. *J. Solid State Chem.* **1986**, *64*, 270.
(3) Ooi, K.; Miyai, Y.; Katoh, S. *Sep. Sci. Technol.* **1986**, *21*, 755.
(4) Ooi, K.; Miyai, Y.; Katoh, S. *Sep. Sci. Technol.* **1987**, *22*, 1779.
(5) Feng, Q.; Kanoh, H.; Miyai, Y.; Ooi, K. *Chem. Mater.* **1995**, *7*, 148.
(6) Feng, Q.; Kanoh, H.; Miyai, Y.; Ooi, K. *Chem. Mater.* **1995**, *7*, 1226.
(7) Feng, Q.; Kanoh, H.; Miyai, Y.; Ooi, K. *Chem. Mater.* **1995**, *7*, 1722.
(8) Thackeray, M. M.; David, W. I. F.; Bruce, P. G.; Goodenough, J. B. *Mater. Res. Bull.* **1983**, *18*, 461.
(9) Thackeray, M. M.; Johnson, P. J.; De Picciotto, L. A.; David, W. I. F.; Bruce, P. G.; Goodenough, J. B. *Mater. Res. Bull.* **1984**, *19*, 179.
(10) Rossouw, M. H.; De Kock, A.; De Picciotto, L. A.; Thackeray, M. M.; David, W. I. F.; Ibberson, R. M. *Mater. Res. Bull.* **1990**, *25*, 173.
(11) Kanoh, H.; Ooi, K.; Miyai, Y.; Katoh, S. *Langmuir* **1991**, *7*, 1841.
(12) Kanoh, H.; Tang, W.; Makita, Y.; Ooi, K. *Langmuir* **1997**, *13*, 6845.
(13) Armstrong, A. R.; Bruce, P. G. *Nature* **1996**, *381*, 499.
(14) Rossouw, M. H.; Thackeray, M. M. *Mater. Res. Bull.* **1991**, *26*, 463.
(15) Shao-Horn, Y.; Hackney, S. A.; Johnson, C. S.; Thackeray, M. M. *J. Electrochem. Soc.* **1998**, *145*, 582.

10.1021/cm000360l CCC: $19.00
Published on Web 09/28/2000

acid delithiation of Li_2MnO_3 have been reported to have a capacity higher than 190 mA·h/g at the first discharge process.[14−16,20] Our recent study shows that the product obtained by quantitative hydrothermal extraction of lithium had excellent structural stability in repetitive host−guest reactions.[20] Lithium extraction from Li_2MnO_3 is one of the most promising methods for preparing new intercalation materials for Li^+.

Previous studies on the lithium extraction from Li_2MnO_3 in an acid solution indicate that it can be expected to form a stable "layer-like" manganese oxide compound by preserving the structural framework of Li_2MnO_3. It has been reported that lithium extraction from Li_2MnO_3 in a 4.5 mol·dm^{-3} H_2SO_4 solution at 34 and 90−115 °C resulted in a hydrated α-MnO_2 and a β-MnO_2-like product, respectively,[15,16] while lithium extraction in an H_2SO_4 solution at 25 °C formed $Li_{2-x}MnO_{3-x/2}$ (Li/Mn = 0.15),[14] for which the preservation of the close-packed oxygen arrangement of Li_2MnO_3 was proposed. Incomplete lithium extraction seems favorable for preserving the structural framework of Li_2MnO_3. To clear up many suppositions, it is necessary to investigate systematically the lithium extraction from Li_2MnO_3.

In the present study, a well-crystallized single Li_2MnO_3 crystal was synthesized by use of LiCl flux, heating at 650 °C. To control quantitatively the lithium extraction, the crystals were subjected to a hydrothermal treatment in H_2SO_4 solutions of various mole ratios ($[H^+]_l/[Li^+]_s$) of H^+ in solution to Li^+ in the Li_2MnO_3. The cleavage behavior of single crystals during lithium extraction was observed by scanning electron microscopy (SEM). Based on those results, a mechanism for the particle cleavage has been proposed.

Experimental Section

Preparation of Starting Li_2MnO_3. The Li_2MnO_3 powder was prepared by the LiCl flux method. A mixture of LiCl (7.2 g) and MnOOH (1.5 g) was placed in a pure alumina crucible with a diameter of 80 mm. The crucible was set in an electric furnace and heated at 650 °C for 4 days. Air was introduced to the furnace at a flow rate of 400 cm^3/min during the heating. A mixture of the crystal plate and powder were obtained after immersing in distilled water, filtering, washing, and drying at 100 °C. The product was then sieved, and the particles between 10 and 30 μm in size were used for the following Li^+ extraction process.

Lithium Extraction from Li_2MnO_3. The Li^+ extraction from Li_2MnO_3 was studied using H_2SO_4 solutions under a hydrothermal condition. An Li_2MnO_3 sample (0.175 g) was added to a 0.01, 0.015, 0.025, 0.05, 0.075, or 0.10 mol·dm^{-3} H_2SO_4 solution (15 cm^3). The added amount of H_2SO_4 corresponds to the mole ratio ($[H^+]_l/[Li^+]_s$) of H^+ in the solution to Li^+ in the Li_2MnO_3 of 0.1, 0.15, 0.25, 0.50, 0.75, and 1.0, respectively. The mixtures were heated in an autoclave at 140 °C for 72 h with intermittent shaking. After the hydrothermal treatment, the solids were filtered, washed with distilled water, and then dried at 80 °C. The Li^+-extracted samples are abbreviated as Ex-0.1, Ex-0.15, Ex-0.25, Ex-0.5, Ex-0.75, and Ex-1, where the numbers correspond to the $[H^+]_l/[Li^+]_s$ ratio.

Chemical Analyses. The lithium and manganese concentrations of the supernatant solutions were determined by atomic absorption spectrometry. Lithium and manganese contents of the starting Li_2MnO_3 and the Li^+-extracted samples were determined after dissolving them in a mixed solution of HCl and H_2O_2. The available oxygen of each sample was determined by the standard oxalic method.[21] The mean oxidation number of manganese (Z_{Mn}) and the oxygen content were calculated from the value of available oxygen. The fraction of lithium extraction (f_{ex}) was calculated as follows.

$$f_{ex} = \frac{\text{amount of } Li^+ \text{ extracted into solution}}{\text{amount of lithium in starting } Li_2MnO_3} \times 100\% \quad (1)$$

The lattice proton contents of the Li^+-extracted samples were estimated from the weight losses between 100 and 400 °C on thermogravimetric curves.[22]

Physical Analyses. X-ray diffraction (XRD) analyses were carried out using a Rigaku-type RINT2500 X-ray diffractometer with a graphite monochromator. The SEM observation was carried out on a JEOL-type JSM-5310 SEM. A nitrogen adsorption−desorption isotherm at 77 K was obtained on a Quantachrome type Autosorb 1-C apparatus with a sample outgassed for 4 h below 10^{-3} mmHg at 200 °C. The surface area was calculated by the Brunauer−Emmett−Teller (BET) method. Thermogravimetric−differential thermal analysis (TG-DTA) curves were obtained on a Shimadzu type (DTG-50) thermal analyzer at a heating rate of 10 K/min.

Results

Characterization of Li_2MnO_3. Lithium and manganese contents of the starting Li_2MnO_3 were 16.9 and 8.5 mmol/g, respectively, and the mean oxidation number of manganese (Z_{Mn}) was 4.0. The chemical formula ($Li_{2.0}MnO_{3.0}$) on the basis of the chemical analyses is the same as the theoretical formula of Li_2MnO_3. A SEM photograph of Li_2MnO_3 showed that it consisted mainly of polyhedral crystals between 10 and 30 μm in size (Figure 1, top). The surface of the particles is smooth. XRD analysis indicated that the crystal system of Li_2MnO_3 is identical with that of a single phase of monoclinic Li_2MnO_3 with a d_{001} value of 4.74 Å (Figure 1, bottom). The TG-DTA curves (TG-DTA curves are given in Figure 5) of Li_2MnO_3 showed no weight change or thermal effect until 1000 °C.

The LiCl flux gives well-crystallized Li_2MnO_3 crystals. It is more stable against heating than other lithium manganese dioxides such as $LiMnO_2$, spinel type $LiMn_2O_4$, or $Li_{1.33}Mn_{1.67}O_4$.[19,23,24]

Lithium Extraction. The starting Li_2MnO_3 was stable against acid treatment at room temperature. Only 0.9 mmol/g of lithium (corresponding to $f_{ex} = 5\%$) was extracted when the starting Li_2MnO_3 (0.1 g) was treated in a 5 mol·dm^{-3} H_2SO_4 solution (50 cm^3) at room temperature for even 16 months. The lithium extractability is markedly lower than that in the literature, in which a significant lithium extraction from Li_2MnO_3 has been found in an acid solution even at 25 and 34 °C.[14,16] The low lithium extractability of the present Li_2MnO_3 may be due to its well-crystallized form.

The lithium extraction and the manganese dissolution were studied under the hydrothermal condition at 140

(16) Shao-Horn, Y.; Ein-Eli, Y.; Robertson, A. D.; Averill, W. F.; Hackney, S. A.; Howard, W. F., Jr. *J. Electrochem. Soc.* **1998**, *145*, 16.
(17) Rossouw, M. H.; Liles, D. C.; Thackeray, M. M. *Mater. Res. Bull.* **1992**, *27*, 221.
(18) Lubin, F.; Lecerf, A.; Broussely, M.; Labat, J. *Powder Source* **1991**, *34*, 161.
(19) Tang, W.; Kanoh H.; Ooi, K. *J. Solid State Chem.* **1999**, *142*, 19.
(20) Tang, W.; Kanoh H.; Ooi, K. *J. Mater. Sci. Lett.*, in press.
(21) Japan Industrial Standard (JIS) M8233, 1969.
(22) Feng, Q.; Miyai, Y.; Kanoh, H.; Ooi, K. *Langmuir* **1992**, *8*, 1861.
(23) Takada, T.; Hayakawa, H.; Kumagai, T.; Akiba, E. *J. Solid State Chem.* **1996**, *121*, 79.
(24) Strobel, P.; Lambert-Andron, B. *J. Solid State Chem.* **1988**, *75*, 90.

Table 1. Analysis Results and Chemical Composition of the Li^+-Extracted Samples

sample	$[H^+]_l/[Li^+]_s$[a]	contents (mmol/g) Li	Mn	H	Z_{Mn}[b]	Li/Mn	H/Mn	chemical composition
Li_2MnO_3		16.9	8.5		4.0_2	2.0		Li_2MnO_3
Ex-0.1	0.10	15.3	8.6	1.7	4.0_1	1.78	0.20	$Li_{1.78}H_{0.20}MnO_{3.0}$
Ex-0.15	0.15	14.6	8.6	2.6	4.0_0	1.70	0.30	$Li_{1.70}H_{0.30}MnO_{3.0}$
Ex-0.25	0.25	13.1	8.7	3.0	3.9_7	1.51	0.34	$Li_{1.51}H_{0.34}MnO_{2.9}$
Ex-0.5	0.50	8.5	9.2	6.0	4.0_1	0.92	0.65	$Li_{0.92}H_{0.65}MnO_{2.8}$
Ex-0.75	0.75	4.5	9.4	7.0	3.9_6	0.48	0.74	$Li_{0.48}H_{0.74}MnO_{2.6}$
Ex-1	1.00	0.2	10.8	3.6	3.9_5	0.02	0.33	$Li_{0.02}H_{0.33}MnO_{2.2}$

[a] $[H^+]_l/[Li^+]_s$: mole ratios of H^+ in solution to Li^+ in Li_2MnO_3. [b] Z_{Mn}: mean oxidation number of manganese.

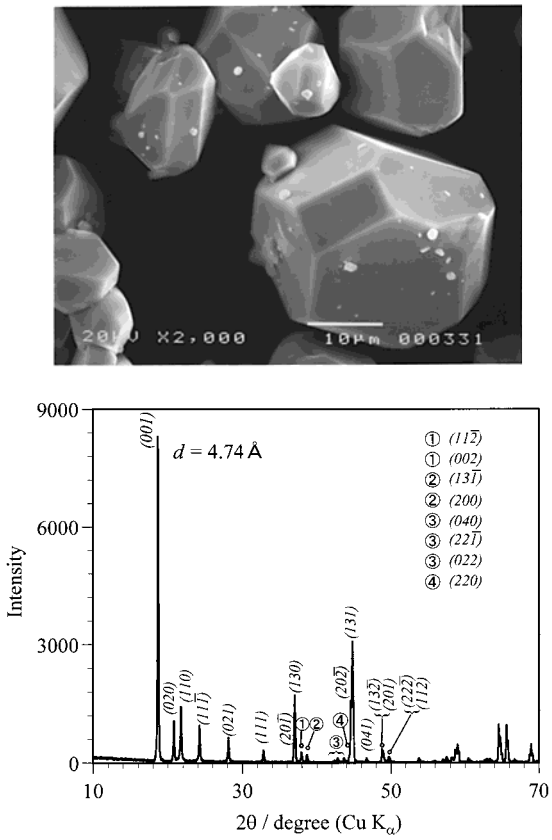

Figure 1. SEM image (top) and XRD pattern (bottom) of starting Li_2MnO_3.

°C in the H_2SO_4 solutions. Manganese dissolution was not detected by the analysis of the supernatant solutions (Mn concentration was less than 10^{-6} mol·dm^{-3}). The lithium concentration in the supernatant solution increased in proportion to the initial H_2SO_4 solution. The acid−base titration of the supernatant solutions showed that the protons in the starting solutions were almost consumed by the hydrothermal treatment. The amounts of Li^+ extracted into solution are plotted as a function of H^+ consumed in Figure 2. Both amounts are equal for all of the samples, indicating that the selective lithium extraction proceeds by consuming an equivalent amount of protons in the solution.

Chemical analysis results of the Li^+-extracted samples are shown in Table 1. The chemical compositions in the last column were calculated from the lithium, manganese, and lattice proton contents and mean oxidation numbers of manganese (Z_{Mn}) of solids. The lithium content decreases while the manganese content increases slightly with an increase in the $[H^+]_l/[Li^+]_s$ ratio. The tetravalent state of manganese in solids shows that the redox reaction does not take place during the

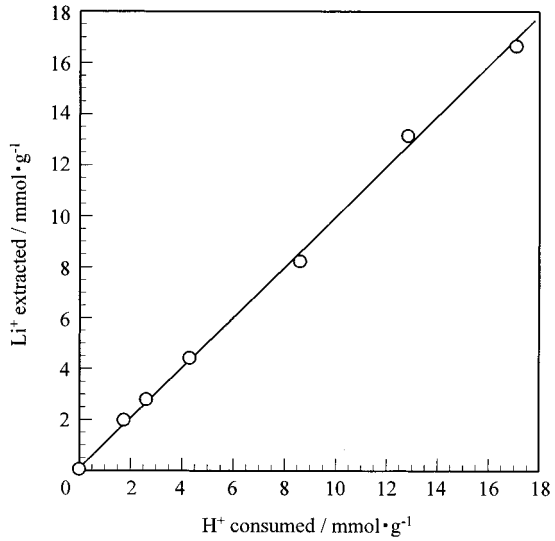

Figure 2. Changes in the amount of Li^+ extracted with the amount of H^+ consumed in solution.

lithium extraction. The lattice proton content of the solids increases with the $[H^+]_l/[Li^+]_s$ ratio up to 0.75 and then decreases. When the changes of the H/Mn ratio are compared with those of Li/Mn ratios, it is found that the amount of H^+ inserted into the solid is almost equal to that of Li^+ extracted for Ex-0.1 and Ex-0.15 but observably smaller for the other samples.

Change in Morphology. No distinguishable change was found for Ex-0.1 and Ex-0.15. However, SEM photographs of Ex-0.25, Ex-0.5, and Ex-0.75 show that they have a unique form; platelike particles are stacked, preserving the outline of the starting Li_2MnO_3 particle (Figure 3a,b). They resemble the starting Li_2MnO_3 particle cut into round slices of different thickness. We have not seen this kind of manganese oxide with such microstructure before. The plane of the plates formed has a polygonal form with the same interior angles as those of the starting Li_2MnO_3 particle (Figure 3a). The thickness of the plates decreases observably with an increase in the $[H^+]_l/[Li^+]_s$ ratio. This indicates that the lithium extraction brings about the cleavage of the Li_2MnO_3 particle when $[H^+]_l/[Li^+]_s \geq 0.25$. No other alien substance was found in Ex-0.25 and Ex-0.5, but a small quantity of rod-shaped crystals was found at the side of the plate in Ex-0.75 (marked with arrows in Figure 3a) while needle-shaped crystals formed on the surface of Ex-1. The stacked-plate structure is stable when $0.25 \leq [H^+]_l/[Li^+]_s \leq 0.75$ but destroyed for Ex-1. Magnified SEM observation was carried out on both the surface and side of the cleaved plate (Figure 3b,c). The image of the side of the plate shows that the plate consists of an aggregate of very thin subplates of

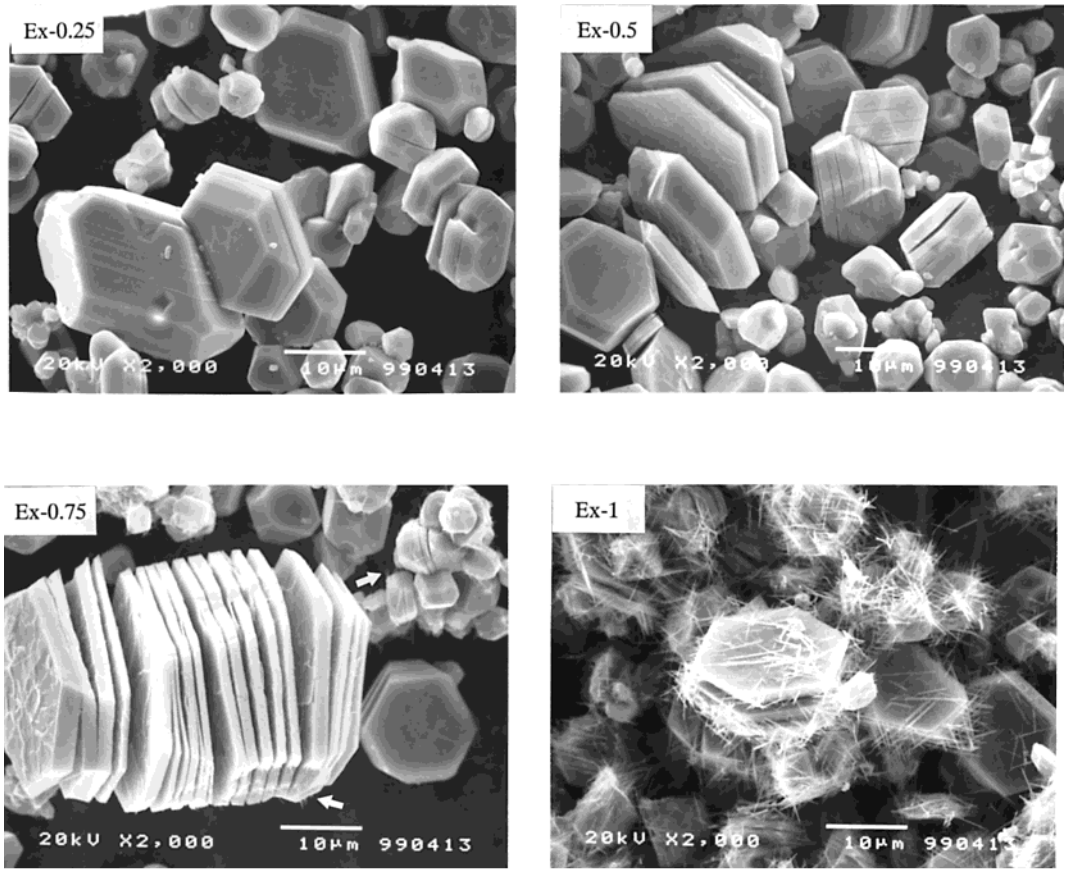
Ex-0.25
20kV X2,000 10μm 990413
Ex-0.5
20kV X2,000 10μm 990413
Ex-0.75
20kV X2,000 10μm 990413
Ex-1
20kV X2,000 10μm 990413

a

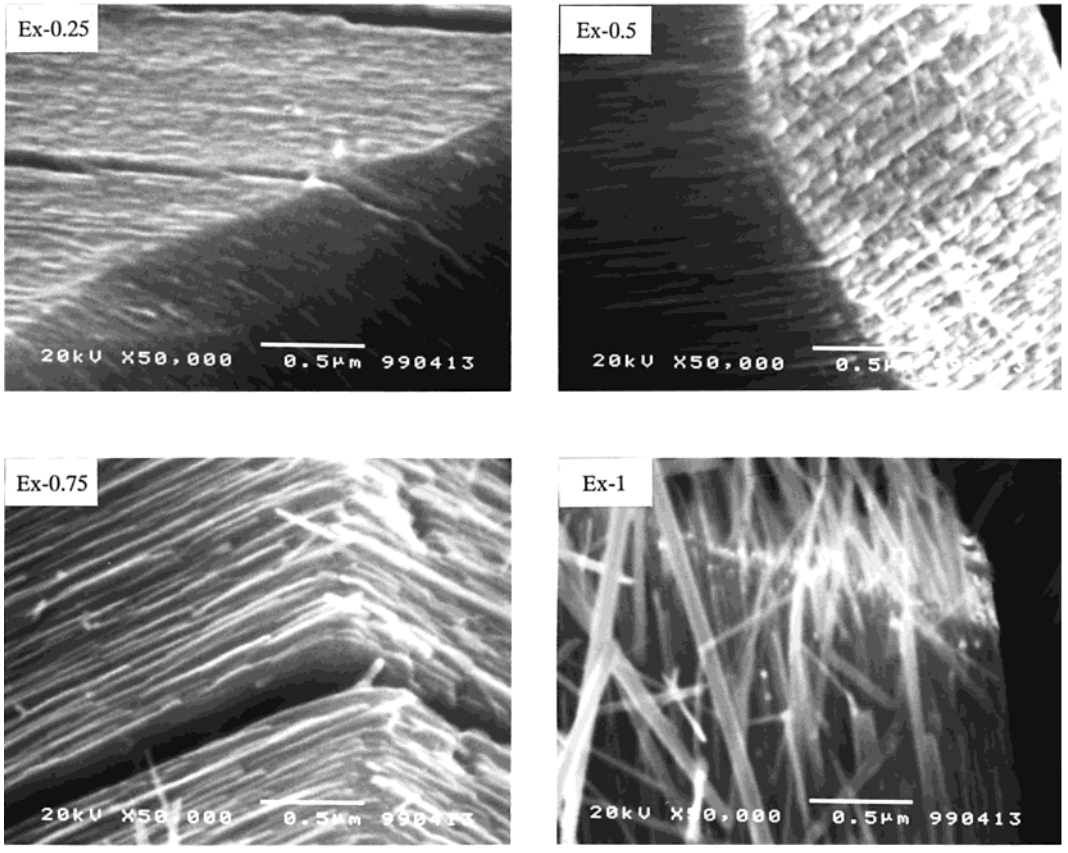
Ex-0.25
20kV X50,000 0.5μm 990413
Ex-0.5
20kV X50,000 0.5μm
Ex-0.75
20kV X50,000 0.5μm 990413
Ex-1
20kV X50,000 0.5μm 990413

b

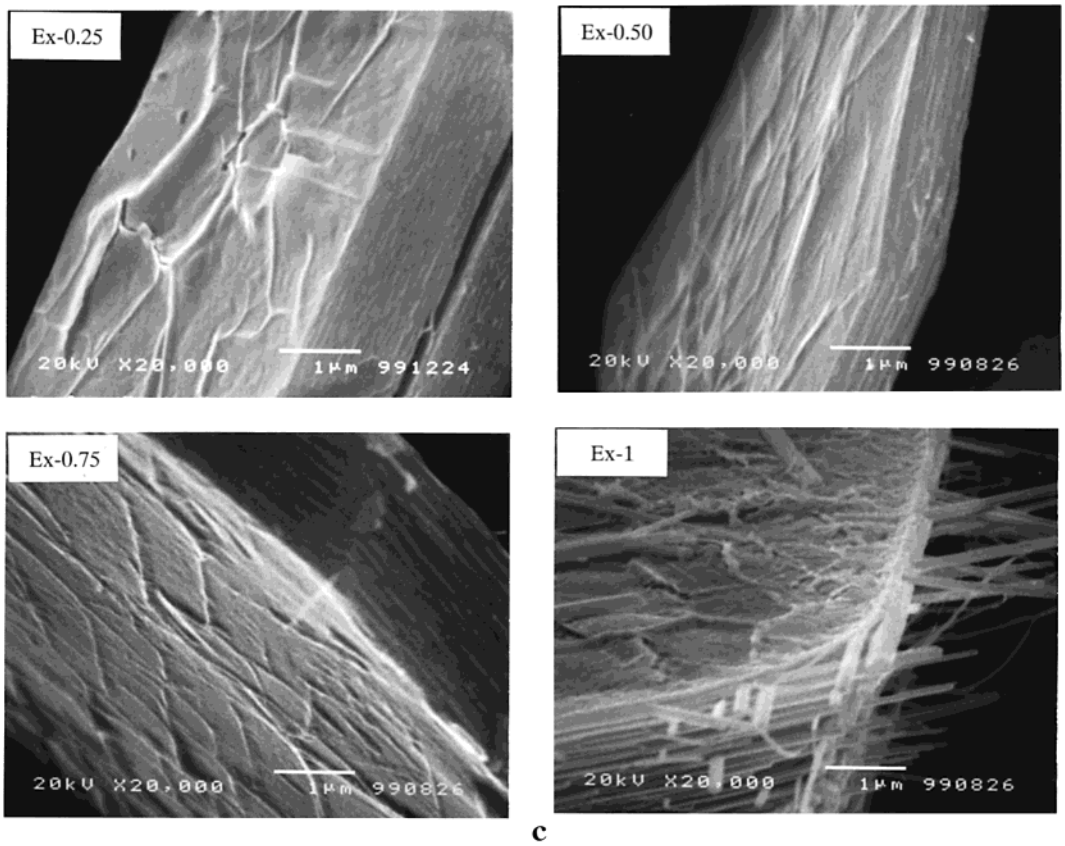

c

Figure 3. (a) SEM images of the Li^+-extracted samples. (b) Magnified SEM images of the side of the plate in the Li^+-extracted samples. (c) Magnified SEM images of the cleaved surface in the Li^+-extracted samples.

nanometer thickness in parallel arrangement (Figure 3b). The thickness of the subplates in Ex-0.25, Ex-0.5, and Ex-0.75 was 10−30 nm. The cracks among subplates become more pronounced with the progression of lithium extraction. The formation of welts was found on cleaved surfaces for Ex-0.25, Ex-0.5, and Ex-0.75, while Ex-1 has a rough surface (Figure 3c). The needle-shaped crystals appear to grow out of the side of the plate in Ex-1.

Change in the Crystal Phase. XRD patterns of the Li^+-extracted samples are given in Figure 4a. The main peaks in Ex-0.15, Ex-0.25, Ex-0.5, and Ex-0.75 are the same as those of the starting Li_2MnO_3 (marked with ●). This indicates that the monoclinic phase of the starting Li_2MnO_3 is preserved as a main phase even after the lithium extraction up to 75%. Two peaks at d = 4.60 and 4.43 Å are observed for the patterns of these samples; they are ascribed to the monoclinic phase with smaller lattice parameters perpendicular to the (001) plane. The pattern for Ex-0.5 shows small portions of hydrated α-MnO_2 (indicated by ○),[15] and that for Ex-0.75, the formation of hydrated α-MnO_2 and γ-MnO_2 phases (▽). This shows that partial structural transformation takes place for Ex-0.5 and Ex-0.75 by the lithium extraction. The XRD pattern of Ex-1 shows that full lithium extraction brings about a structural change from the monoclinic phase to γ-MnO_2. The final crystal phase at the full lithium extraction is different from those in the literature,[11,12] where the final products of the β-MnO_2-like phase and a hydrated α-MnO_2 have been reported.

Thin film XRD analyses were carried out to identify the orientation of the platelike particles (Figure 4b). The Li^+-extracted samples were dispersed in thinner on the surface of a glass holder. Three main peaks at d_{001} = 4.73 Å and d = 4.60 and 4.42 Å are strengthened in the patterns of Ex-0.25, Ex-0.5, and Ex-0.75. This shows that the plate in Figure 3a contains planes parallel to the (001) crystal plane. The peak at d = 7.04 Å for Ex-0.25 and d = 7.10 Å for Ex-0.5 and Ex-0.75 in Figure 4b is more distinguishable than that in Figure 4a for three samples. This suggests that the hydrated α-MnO_2 phase is formed on the samples of the plate.

Thermal Behavior. TG-DTA curves of the starting Li_2MnO_3 and the Li^+-extracted samples are given in Figure 5. The TG curves show weight losses above 100 °C for the Li^+-extracted samples. These weight losses can be characterized as the dissipation of water molecules by the condensation of lattice OH groups,[22] indicating the presence of the Li^+/H^+ ion-exchange reaction. Two endothermic peaks are observed around 200 °C for samples Ex-0.15 and Ex-0.25, while there are two peaks separated at around 150 and 230 °C for samples Ex-0.5 and Ex-0.75. All of the peaks are accompanied by weight losses in the TG curves. These results suggest the presence of two kinds of OH sites with different thermal stability.

Mesoporous Structure. The nitrogen adsorption−desorption isotherms type for Ex-0.25, Ex-0.5, Ex-0.75, and Ex-1 can be classified as BDDT type IV (Figure 6),[25] which is observed for mesoporous materials consisting of aggregates of platelike particles with slit-shaped pores,[25,26] such as naturally occurring sodium-rich

(25) Sing, K. S. W.; Everett, D. H.; Haul, R. A.; Moscou, L.; Siemieniewska, T. *Pure Appl. Chem.* **1985**, *57*, 603.

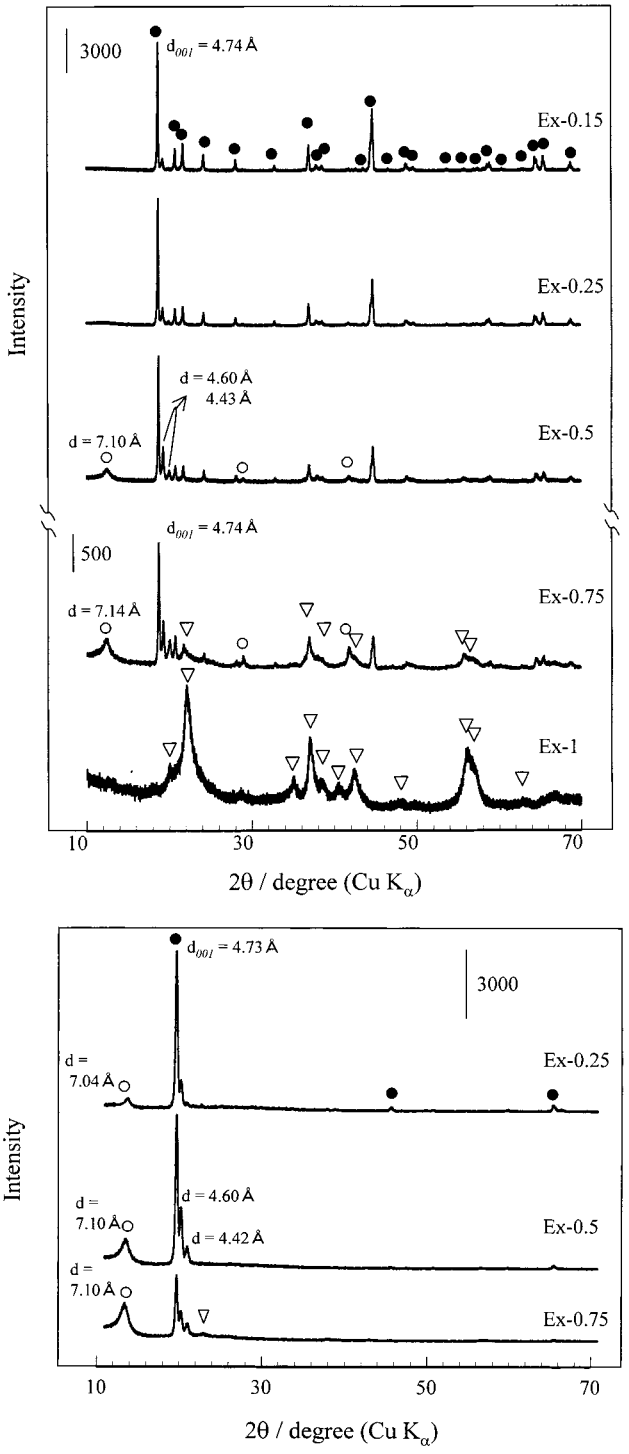

Figure 4. (a) XRD patterns of the Li^+-extracted samples (●, Li_2MnO_3; ○, hydrated α-MnO_2; ▽, γ-MnO_2). (b) Thin film XRD patterns of the Li^+-extracted samples. The thin film sample was mounted on the surface of the reverse side of a glass holder.

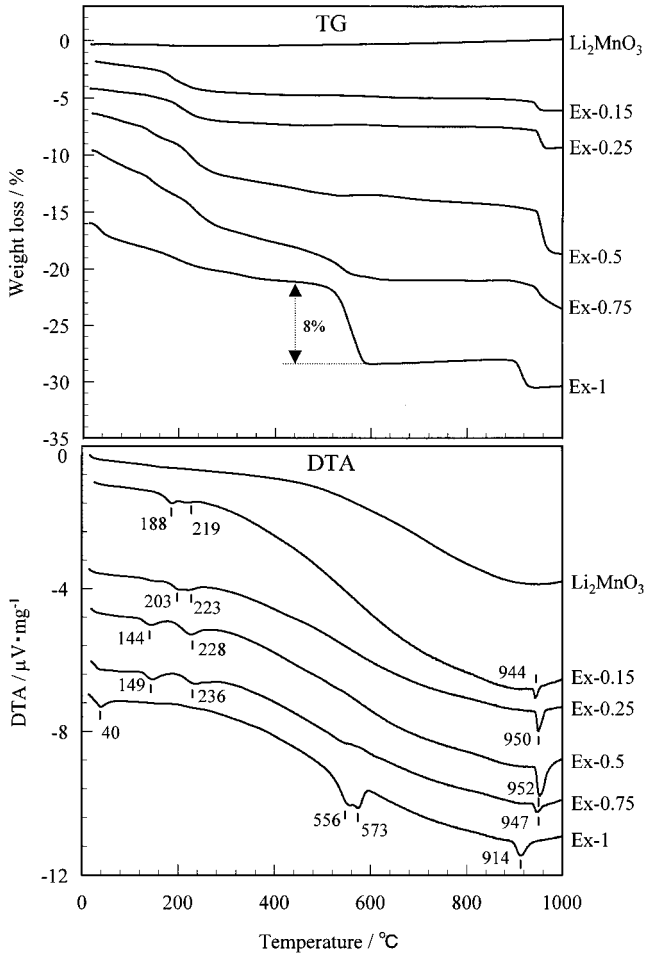

Figure 5. TG-DTA curves of the starting Li_2MnO_3 and the Li^+-extracted samples.

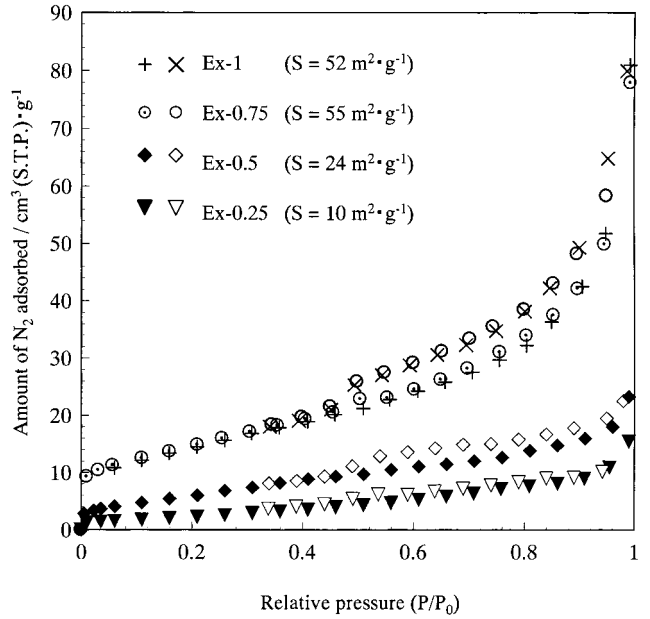

Figure 6. Nitrogen adsorption−desorption isotherms of the Li^+-extracted samples (S = BET surface area).

montmorillonite[27] and halloysite.[28] This suggests that Ex-0.25, Ex-0.5, Ex-0.75, and Ex-1 have slit-shaped mesopores. The BET surface areas are less than 1 $m^2 \cdot g^{-1}$ for the starting Li_2MnO_3, Ex-0.1, and Ex-0.15 and 10, 24, 55, and 52 $m^2 \cdot g^{-1}$ for Ex-0.25, Ex-0.5, Ex-0.75, and Ex-1, respectively. This shows that the lithium extraction develops the cleavage of the starting particle to form new surfaces. We can conclude from these results that hydrothermal lithium extraction from well-

(26) Gregg, S. J.; Sing, K. S. W. *Adsorption, Surface Area and Porosity*; Academic Press: London, 1982; p 111.
(27) Barrer, R. M.; MacLeod, D. M. *Trans. Faraday Soc.* **1954**, *50*, 980.
(28) Gregg, S. J.; Langford, J. F. *J. Chem. Soc., Faraday Trans. 1* **1977**, *73*, 747.

crystallized Li_2MnO_3 gives a manganese oxide with slit-shaped mesopores.

Discussion

Chemical Reaction of Lithium Extraction from the Li_2MnO_3 Particle. For the lithium extraction from Li_2MnO_3, Rossouw and Thackeray have proposed that Li_2O dissolution is the major reaction,[14] while Lubin et al. proposed a Li^+/H^+ ion-exchange reaction.[18] The present results show that both the Li^+/H^+ ion exchange and lithium dissolution take place for lithium extraction from well-crystallized Li_2MnO_3. Because the amount of H^+ inserted is equal to that of Li^+ extracted for samples Ex-0.1 and Ex-0.15, only the Li^+/H^+ ion-exchange reaction progresses for these two samples as follows:

$$Li_2MnO_3(s) + xH^+(l) \rightarrow Li_{2-x}H_xMnO_3(s) + xLi^+(l) \quad (2)$$

where the notations s and l refer to the species in the solid and liquid phases, respectively. The Li^+/H^+ ion-exchange reaction progresses topotactically, preserving the monoclinic structure of Li_2MnO_3. The H^+ contents of the other Li^+-extracted samples, however, are considerably smaller than those expected from the amounts of Li^+ extracted, assuming a Li^+/H^+ ion exchange (Table 1). The smaller H^+ content can be ascribed to the dissolution of lithium as Li_2O, in addition to the Li^+/H^+ ion exchange. The lithium dissolution reaction can be written as follows.

$$Li_2MnO_3 + 2yH^+ \rightarrow Li_{2(1-y)}MnO_{3-y} + 2yLi^+ + yH_2O \quad (3)$$

Lithium dissolution accompanies a loss of lattice oxygen. The fraction of H^+/Li^+ ion exchange (f_{ion}) and the fraction of lithium dissolution (f_{diss}) can be calculated by assuming that the amount of lithium extraction is the total amount of H^+/Li^+ ion exchange and lithium dissolution, as follows.

$$f_{ion} = \frac{\text{amount of } H^+ \text{ in solid (mmol}\cdot g_{Li_2MnO_3}^{-1})}{\text{amount of lithium in starting } Li_2MnO_3 \text{ (mmol}\cdot g_{Li_2MnO_3}^{-1})} \times 100\% \quad (4)$$

$$f_{diss} = f_{ex} - f_{ion} \quad (5)$$

The amount of H^+ in the solid was converted to millimoles per gram of starting Li_2MnO_3 for comparison with the amount of Li^+ extracted. The values of f_{ex}, f_{diss}, and f_{ion} are given in Figure 7. The f_{ion} value increases with the $[H^+]_l/[Li^+]_s$ ratio up to 0.75 and then decreases, while the f_{diss} value increases monotonically in the range $[H^+]_l/[Li^+]_s \geq 0.25$. The f_{diss} values are smaller than the f_{ex} values for Ex-0.25 and Ex-0.5 but slightly larger than those for Ex-0.75. The lithium dissolution becomes the main reaction at $[H^+]_l/[Li^+]_s = 1$.

Mechanism for the cleavage of the Li_2MnO_3 particle. Li_2MnO_3 has a rock salt structure with a close-packed oxygen anion array in which layers of Li atoms ([Li]) and layers of a mixture of Li and Mn atoms (Mn:Li = 2:1, [Mn_2Li]) alternate with one another along the direction perpendicular to the *c* axis with intervening layers of oxygen (Figure 8, right).[24] Three kinds of Li^+ sites are present in Li_2MnO_3: at 2b sites in the [Mn_2-Li] layer and at 2c and 4h sites in the [Li] layer. It is reasonable to consider that the initial Li^+/H^+ ion exchange proceeds through the 2c and 4h Li^+ sites of [Li] layers, because the LiO_6 octahedra at 2c and 4h sites in the [Li] layer are unstable because of their distorted form and the lithium atoms can migrate easily to the solid surface through the [Li] layer without interference from Mn atoms. Two endothermic peaks in the DTA curves of the Li^+-extracted samples when $[H^+]_l/[Li^+]_s$ ratio $\leq$ 0.75 (Figure 5) are possibly attributed to the two kinds of hydroxyl groups formed by the Li^+/H^+ ion-exchange reaction at 2c and 4h sites. The OH groups formed by the Li^+/H^+ ion-exchange reaction prefer an orientation toward nearest-neighbor oxygen O−O (Figure 8), similar to the case of spinel-type lithium manganese oxides.[29,30] The length of OH has been reported as 0.93−0.98 Å, which is about one-third of that (3.05 Å) of the O−O bond. Therefore, the Li^+/H^+ ion exchange may bring the lattice contraction along the *c* axis to give the small d_{001} values of 4.60 and 4.43 Å as identified in the XRD patterns of Figure 4a.

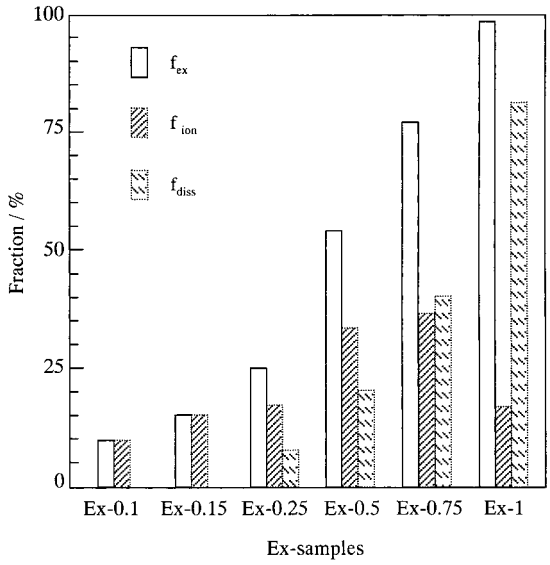

Figure 7. Fractions of lithium extraction, H^+/Li^+ ion change, and lithium extraction for the Li^+-extracted samples.

The cleavage of the particle by the lithium extraction is schematically illustrated in Figure 9. The Li^+/H^+ ion-exchange reaction starts on the surface of the Li_2MnO_3 particle perpendicular to the (001) plane (Figure 9b), accompanied by the contraction of the lattice. The lattice contraction in the Li^+-exchanged phase produces distortion and strong stress at the interface between the unreacted Li_2MnO_3 and the Li^+-exchanged phase. When the stress exceeds the hydrogen-bonding energy following further lithium extraction, the cracks are formed at appropriate intervals (Figure 9c), as shown in the SEM image of Ex-0.25. Once the crack is formed, the lithium extraction progresses preferably from the top of the crack because the point of the crack is in a highly active state. In addition, the dissolution of Li_2O may

(29) Ammundsen, B.; Roziere, J.; Islam, M. S. *J. Phys. Chem. B* **1997**, *101*, 8156.
(30) Ammundsen, B.; Burns, G. R.; Jones, D. J.; Roziere, J. *J. Chem. Mater.* **1996**, *8*, 2799.

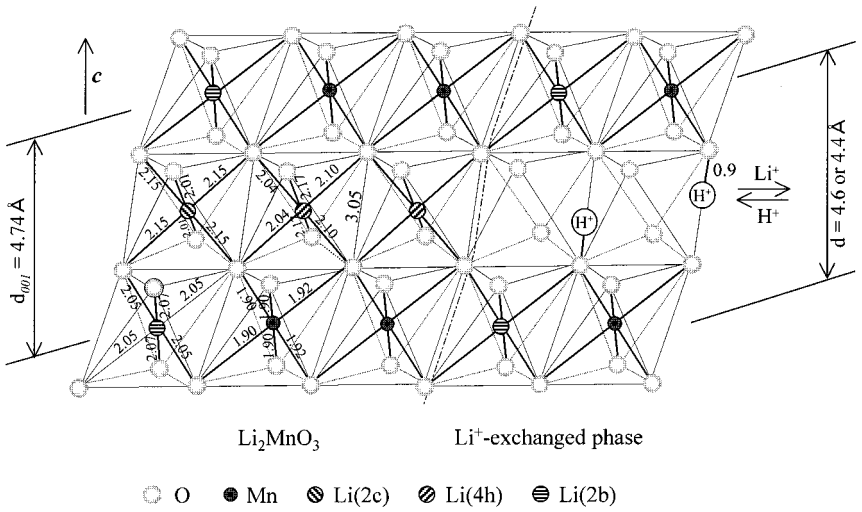

Figure 8. Structure of Li_2MnO_3 and after the Li^+/H^+ ion-exchange reaction (unit of length is angstroms).

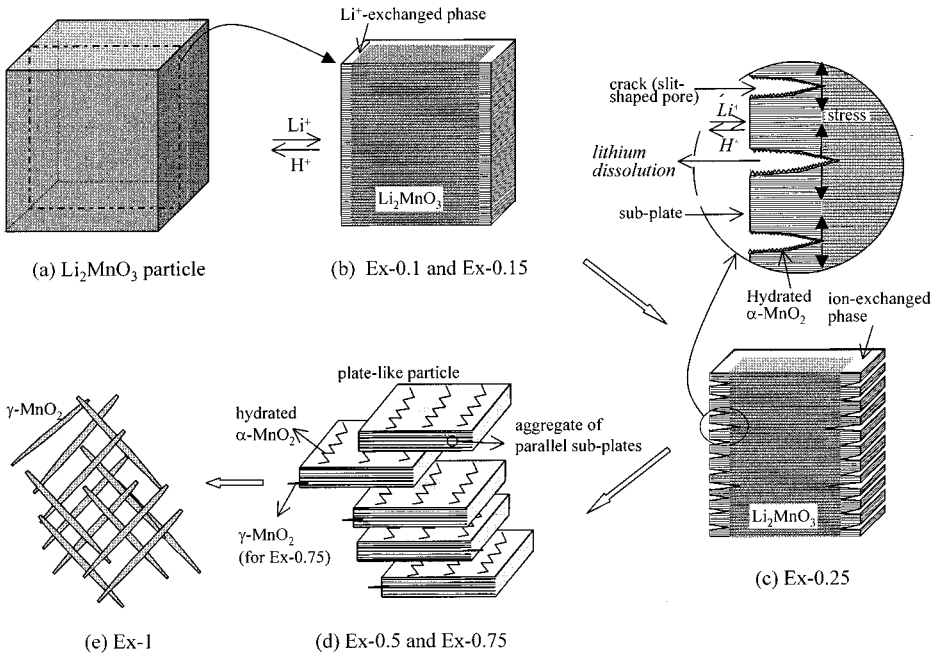

Figure 9. Morphological image of the particle cleavage.

progress more easily on the cleaved surface because the cleaved surface is more active than the conventional particle surface. The hydrated α-MnO_2 phase, observed on the surface of the platelike particles by thin film XRD analyses, can be ascribed to the product formed as a result of the Li_2O dissolution from Li_2MnO_3. These two reactions accelerate the growth of the cracks, consequently producing the subplate. Further growth of the cracks results in the cleavage of the particle to produce stacked platelike particles (Figure 9d), as shown in the SEM images of Ex-0.5 and Ex-0.75.

The nitrogen adsorption−desorption isotherms show that the BET surface area of the Li^+-extracted sample increases with the progress of lithium extraction when $[H^+]_l/[Li^+]_s \leq 0.75$. This can be ascribed to the formation of new surfaces during the cleavage of the starting Li_2MnO_3 particle. It can be calculated that cleavage from hexastyle Li_2MnO_3 particles with a diagonal length of hexagon of 20 μm and a height of 20 μm to the hexagonal plate with a thickness of 10 nm increases the surface area to 42 m^2/g (the theoretical density of Li_2MnO_3 is calculated as 4.8 g/cm^3 from the cell parameters of a = 4.94 Å, b = 8.53 Å, c = 5.03 Å, and β = 109.5°). The BET surface area (55 g/cm^3) of Ex-0.75 is larger than the calculated value, probably because of its rough surface. This shows that subplates extend to the inside of the solid. Between the subplates, slit-shaped mesopores are formed.

Phase Transformation. We consider that the phase transformation to hydrated α-MnO_2 proceeds on the cleaved surface by lithium dissolution as shown in Figure 9c. The dissolution of lithium can be rewritten from eq 3 as follows.

$$Li_2MnO_3 + 2H^+ \rightarrow MnO_2 \cdot H_2O + 2Li^+ \qquad (6)$$

The reaction (6) forms hydrated α-MnO_2 on the surface of the plates. Therefore, the dissolution of lithium does not destroy the basic monoclinic structure in the solids even for Ex-0.75, in which the value of f_{diss} reaches 39% for a loss of 20% of lattice oxygen. We note that extent of lithium dissolution increases with an

increase of the BET surface area, and the ratios of the extent of lithium dissolution to BET area are 0.08, 0.1, and 0.1 mmol/m^2 for Ex-0.25, Ex-0.5, and Ex-0.75. The ratios correspond to the amount of lithium in 2−3 layers of [Li] and of [Mn_2Li] at the surface, respectively.

The phase formation to γ-MnO_2 in Ex-0.75 and Ex-1 proceeds through the dissolution of lithium from 2b sites in the [Mn_2Li] layer. Because 2c and 4h lithium sites in the [Li] layer account for 75% of the total lithium in Li_2MnO_3, the dissolution of lithium from 2b sites in the [Mn_2Li] layer starts from $[H^+]_l/[Li^+]_s = 0.75$ for Ex-0.75 and becomes predominant for Ex-1. This destroys the [Mn_2Li] layered structure, causing structural transformation from layered to tunnel type. The lithium dissolution forms a few rod-shaped γ-MnO_2 crystals at the sides of plates for Ex-0.75 (Figure 9d) and a single phase of γ-MnO_2 crystals for Ex-1 (Figure 9e).

Conclusions

Hydrothermal treatment of well-crystallized Li_2MnO_3 results in the selective extraction of lithium by both Li^+/H^+ ion exchange and a Li_2O dissolution mechanism. Lithium extraction brings about cleavage of the particles; manganese oxide in the form of stacked plates can be obtained. The technique of selective extraction is a unique method for the preparation of novel manganese oxide porous crystals.

CM000360L